

---

## ORTHOGONAL COLLOCATION ON FINITE ELEMENTS USING QUINTIC HERMITE BASIS

P. SINGH, N. PARUMASUR AND C. BANSILAL

*Received 21 August, 2020; accepted 24 March, 2021; published 16 July, 2021.*

UNIVERSITY OF KWAZULU-NATAL, SCHOOL OF MATHEMATICS STATISTICS AND COMPUTER SCIENCES,  
PRIVATE BAG X54001, DURBAN, 4000, SOUTH AFRICA.

singhprook@gmail.com  
parumasurn1@ukzn.ac.za  
christelle18@gmail.com

**ABSTRACT.** In this paper we consider the orthogonal collocation on finite elements (OCFE) method using quintic Hermite (second degree smooth) basis functions and use it to solve partial differential equations (PDEs). The method is particularly tailored to solve third order BVPS and PDEs and to handle their special solutions such as travelling waves and solitons, which typically is the case in the KdV equation. The use of quintic polynomials and collocation using Gauss points yields a stable high order superconvergent method. OCFE using quintic Hermite basis is optimal since it is computationally more efficient than collocation methods using (first degree smooth) piecewise-polynomials and more accurate than the (third degree smooth) B-splines basis. Various computational simulations are presented to demonstrate the computational efficiency and versatility of the OCFE method.

*Key words and phrases:* OCFE; Quintic Hermite splines; Solitons; KdV equation.

*2010 Mathematics Subject Classification.* Primary 65L10, 65M70, 65N35.

## 1. INTRODUCTION

Orthogonal collocation on finite elements (OCFE) is a useful and versatile method for solving many problems occurring in science and engineering applications. The method, originally developed in chemical engineering [11, 15, 3], is an efficient numerical tool for handling boundary value problems (BVPs), partial differential (PDEs) and optimal control problems, having steep solution profiles and moving fronts, such as axial dispersion models. Furthermore, nonlinear problems with variable coefficients and mixed boundary conditions are easily handled. The OCFE method is a variant of the method of weighted residuals and is simpler to use than the Galerkin method which is based on a variational formulation. A similar technique, called Orthogonal Spline Collocation (OSC) [14, 13, 6] is based on the latter formulation. The OCFE method primarily arose as an alternative for global collocation methods, in which the solution is sought over the entire computational domain, and using high order polynomials results in oscillations in the approximation. In OCFE the approximation is constrained to smaller subintervals referred to as finite elements. An added advantage of OCFE is that derivative approximations are readily available and this may be useful information in practical applications. In the literature, OCFE employing Lagrange [11, 2, 3] and cubic Hermite basis [15, 16, 17] are well developed and usually efficient for solving second order problems. In this paper we focus on OCFE using quintic Hermite basis which is suitable for solving third order problems. The use of quintic polynomials yield high order stable methods whilst collocation using Gauss points yield fast convergence, sometimes referred to as superconvergence. Furthermore, the resulting matrix vector systems have sparse representations (matrices with block-diagonal structure). We derive the Hermite quintic basis and use it in the OCFE method to solve both linear and nonlinear third order BVPs, linear and nonlinear PDEs, including Burgers' equation and the third order KdV equation. It is clearly demonstrated that the method is computationally efficient in solving problems having traveling wave and soliton solutions. The flexibility of OCFE is further evident when solving nonlinear BVPs and PDEs. The discretization yields either nonlinear equations or a set of differential algebraic equations (DAEs), which may be very accurately solved using either NLsol or DASSL solvers in the Julia programming environment. We also present an alternative strategy using quasilinearization method to manage the time integration process economically. The present OCFE method using quintic Hermite splines is an optimal method for solving third order BVPs and PDEs since it is more efficient than  $C^1$  OSC (see [7]) and more accurate than  $C^3$  B-splines (see [10]).

## 2. QUINTIC HERMITE BASIS FUNCTIONS

We seek a basis for  $P_5$ , the vector space of polynomials of degree  $\leq 5$  on the interval  $[x_i, x_{i+1}]$ . There are six such functions and we denote them by  $H_k$ ,  $k = 1, 2, \dots, 6$ . We further stipulate their function and derivative values at the end points  $x_i$  and  $x_{i+1}$  as follows:

$$(2.1) \quad H_k^{(p)}(x_i) = \frac{\delta_{k,p+1}}{h^p}, \quad H_k^{(p)}(x_{i+1}) = 0, \quad H_{k+3}^{(p)}(x_i) = 0, \quad H_{k+3}^{(p)}(x_{i+1}) = \frac{\delta_{k,p+1}}{h^p},$$

where  $k, p + 1 \in \{1, 2, 3\}$  and  $\delta_{i,j}$  is the well-known Kronecker delta symbol.

It is convenient to transform to the variable  $z \in [0, 1]$  defined by

$$(2.2) \quad z = \frac{x - x_i}{x_{i+1} - x_i} = \frac{x - x_i}{h},$$

where  $h$  is the uniform interval length. As  $x$  varies from  $x_i$  to  $x_{i+1}$ ,  $z$  varies from 0 to 1. The interpolatory conditions in (2.1) transform naturally in the variable  $z$  to

$$H_k^{(p)}(0) = \delta_{k,p+1}, \quad H_k^{(p)}(1) = 0, \quad H_{k+3}^{(p)}(0) = 0, \quad H_{k+3}^{(p)}(1) = \delta_{k,p+1}.$$

These conditions enable the unique derivation of the  $H_k(z)$ ,  $k = 1, 2, \dots, 6$ . The polynomial  $H_3(z)$  has a triple zero at  $z = 1$  and therefore has the form of  $H_3(z) = (z - 1)^3q(z)$ , where  $q(z)$  is quadratic in  $z$ . Using the remaining three conditions,  $H_3^{(p)}(0) = 0$ ,  $p = 0, 1$  and  $H_3^{(2)}(0) = 1$ , it is a simple exercise to determine  $q(z)$ . Using this approach, the polynomials  $H_1(z)$ ,  $H_2(z)$  and  $H_3(z)$  are derived and displayed in equations (2.3)-(2.5)

$$(2.3) \quad H_1(z) = (1 - z)^3(6z^2 + 3z + 1),$$

$$(2.4) \quad H_2(z) = (1 - z)^3(3z^2 + z),$$

$$(2.5) \quad H_3(z) = (1 - z)^3 \left( \frac{1}{2}z^2 \right).$$

By using symmetry/antisymmetry, one can show that

$$H_4(z) = H_1(1 - z), \quad H_5(z) = -H_2(1 - z), \quad H_6(z) = H_3(1 - z).$$

It is easy to check that the set  $\{H_i(z), i = 1, 2, \dots, 6\}$  forms a basis for  $P_5$  on  $[0, 1]$ . In the left panel in Figure 1, we illustrate these basis functions on  $[x_i, x_{i+1}]$ .

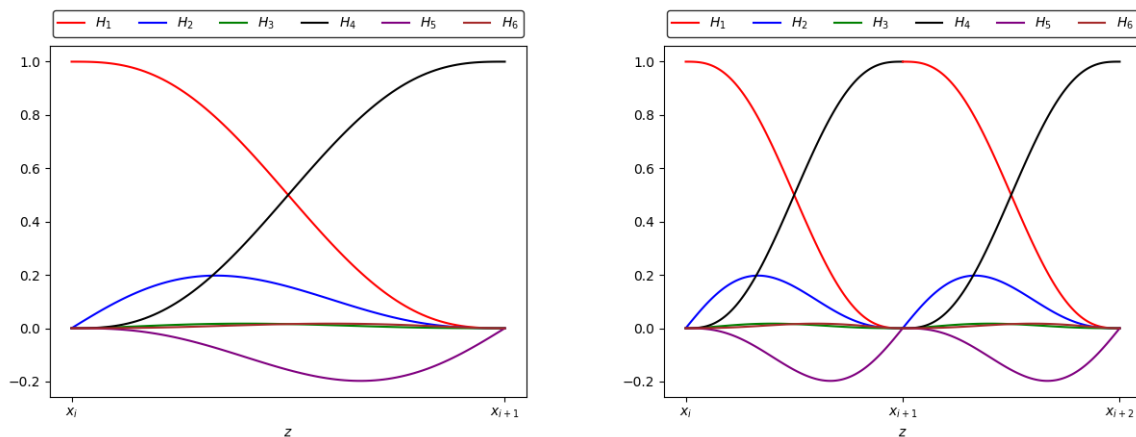


Figure 1: Basis Functions and their representation across successive intervals.

### 3. OCFE METHOD

We consider solving third order BVPs in one spatial variable  $x$ , on the domain  $[a, b]$  of the form

$$(3.1) \quad \alpha(x)y'''(x) + \beta(x)y''(x) + \gamma(x)y'(x) + \eta(x)y(x) = f(x),$$

$$(3.2) \quad y(a) = \theta_1, \quad y(b) = \theta_2, \quad y'(a) = \theta_3.$$

Here, we assume that  $\alpha(x), \beta(x), \gamma(x), \eta(x) \in C^3(a, b)$ . Firstly the domain  $[a, b]$  is divided into  $N$  subintervals or elements of spacing  $h = \frac{b-a}{N}$ , by placing the dividing points or nodes,  $x_i$ ,  $i = 1, 2, \dots, N + 1$ , as illustrated in figure 2. We shall refer to this discretization as the mesh  $\Delta$ .

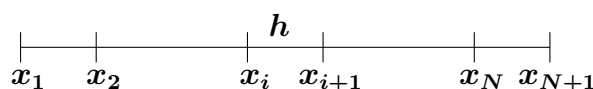


Figure 2: Mesh  $\Delta$

Here  $x_1 = a$  and  $x_{N+1} = b$  coincide with the left and right hand boundaries, respectively. This differs from global orthogonal collocation where the domain is not subdivided and instead higher order polynomials are used to achieve greater accuracy. The  $i_{th}$  element  $[x_i, x_{i+1}]$  is mapped to  $[0, 1]$  by using a transformation of the form (2.2). We assume that the approximate solution in the  $i_{th}$  element is given by

$$Y^i(x) = Y^i(z) = \sum_{k=1}^6 a_k^i H_k^i(z),$$

and is represented in the  $(i + 1)_{st}$  element by

$$Y^{i+1}(x) = Y^{i+1}(z) = \sum_{k=1}^6 a_k^{i+1} H_k^{i+1}(z).$$

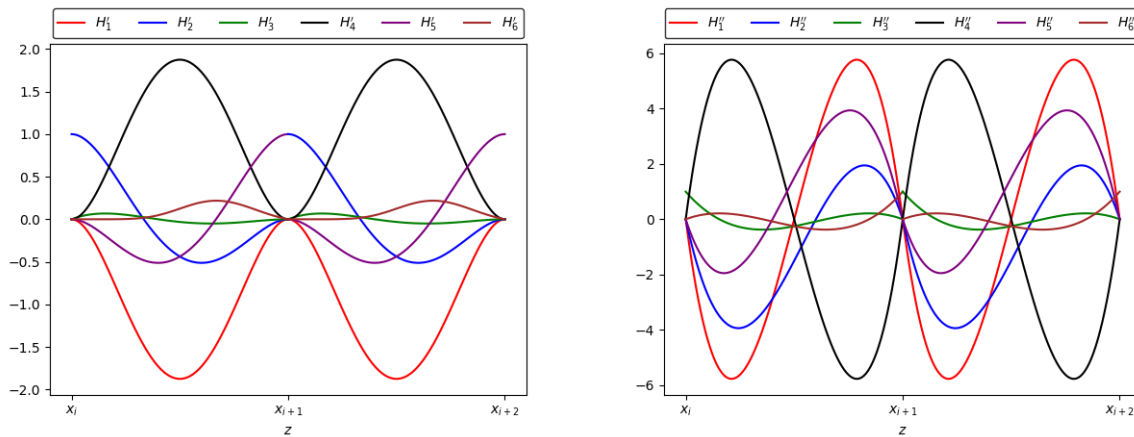


Figure 3: 1st and 2nd derivatives of the basis functions on successive intervals

The basis functions, their first derivatives and their second derivatives are plotted across both the  $i_{th}$  and  $(i + 1)_{st}$  elements and illustrated in the right panel in Figure 1 and in Figure 3, respectively. We observe continuity at  $x_{i+1}$  for the basis functions, their first and their second derivatives. From Figure 3 we deduce that the third derivatives are not all continuous at  $x_{i+1}$  since there exists cusps in the figure. The continuity of the basis functions and their first and second derivatives have some interesting consequences on the coefficients of the solutions in the successive elements.

In order to obtain a smooth solution that is  $C^2$  continuous, we enforce the condition

$$Y^i(x_{i+1}) = Y^{i+1}(x_i),$$

which is equivalent, in the variable  $z$ , to

$$Y^i(1) = Y^{i+1}(0).$$

This implies that  $a_1^{i+1} = a_4^i$ . The continuity of the first and second derivatives at  $x_{i+1}$  is equivalent to

$$\left. \frac{dY^{(i)}}{dz} \right|_{z=1} = \left. \frac{dY^{(i+1)}}{dz} \right|_{z=0}, \quad \left. \frac{d^2Y^{(i)}}{dz^2} \right|_{z=1} = \left. \frac{d^2Y^{(i+1)}}{dz^2} \right|_{z=0},$$

and yields  $a_2^{i+1} = a_5^i$ ,  $a_3^{i+1} = a_6^i$ , respectively.

Hence the first three coefficients in the  $(i + 1)_{st}$  interval coincide with the last three coefficients in the  $i_{th}$  interval. This repetitive pattern continues as we proceed to successive elements. Thus, we may represent the solution in the  $i_{th}$  element by

$$(3.3) \quad Y(z) = \sum_{k=1}^6 a_{k+3(i-1)} H_k(z),$$

where we write  $H_k(z)$  for  $H_k^i(z)$  bearing in mind that  $H_k(z)$  is a function of  $i$  and that we have dropped the superscript  $i$  from  $Y^i(z)$ . With this labeling of the coefficients we are automatically ensuring that the solution and its first and second derivatives are continuous at the nodes.

**Remark 3.1.** Substituting  $z = 0$  and  $z = 1$  into (3.3), its derivative and its second derivative, we can show that  $Y(x_i) = a_{3i-2}$ ,  $hY'(x_i) = a_{3i-1}$  and  $h^2Y''(x_i) = a_{3i}$ ,  $i = 1, 2, \dots, N + 1$ . Thus every third coefficient beginning from  $a_1$  is an approximation to the solution at the nodes. Similarly every third coefficient beginning from  $a_2$  scaled by  $h$ , is an approximation to the derivative at the nodes. Likewise, every third coefficient beginning from  $a_3$  scaled by  $h^2$  represents an approximation to the second derivative at the nodes.

Next we outline the OCFE method for solving (3.1)-(3.2). Substituting (3.3) into (3.1) results in the following system of equations:

$$(3.4) \quad \sum_{k=1}^6 \left[ \frac{\alpha(z)}{h^3} H_k'''(z) + \frac{\beta(z)}{h^2} H_k''(z) + \frac{\gamma(z)}{h} H_k'(z) + \eta(z) H_k(z) \right] a_{k+3(i-1)} = f(z),$$

$i = 1, 2, \dots, N$ . The boundary conditions

$$y(a) = Y(0) = \sum_{k=1}^6 a_k H_k(0) = \theta_1, \quad y(b) = Y(1) = \sum_{k=1}^6 a_{k+3(N-1)} H_k(1) = \theta_2$$

yields  $a_1 = \theta_1$ ,  $a_{3N+1} = \theta_2$ , respectively. Similarly, the boundary condition

$$y'(a) = hY'(0) = h \sum_{k=1}^6 a_k H_k'(0) = \theta_3$$

yields  $a_2 = \theta_3/h$ . There are  $3N + 3$  unknowns in equation (3.4). Given that we have three boundary conditions, we thus require  $3N$  additional conditions in order to solve the problem uniquely. We choose three collocation points  $r_1, r_2, r_3$  in the  $N$  intervals. The  $r_j$  are chosen as the zeros of the third degree Legendre polynomial, shifted to the interval  $[0, 1]$ . These can be shown to be the optimal choice for collocation points. The collocation points  $r_j, j = 1, \dots, 3$  are then substituted for  $z$  in each element in equation (3.4) to give the remaining  $3N$  linear equations. The matrix vector system, of size  $(3N + 3) \times (3N + 3)$ , has the form  $Aa = f$  where  $A$  has the form  $(N = 3)$



By taking the ratio of the equations in (3.8) we obtain

$$\alpha = |D^p(y - Y)(x_j)|_h / |D^p(y - Y)(x_j)|_{\frac{h}{2}} \approx 2^n,$$

from which the order of convergence

$$(3.9) \quad n^p(h) \approx \ln(\alpha) / \ln(2)$$

is estimated. A similar technique is used to estimate the global convergence rate in (3.7).

**Example 3.1.** *We now consider the BVP*

$$y'''(x) + 2y'(x) = -980 \cos(10x)$$

$$y(0) = 0, y'(0) = 10, y(1) = \sin(10).$$

The conditions of Theorem 3.1 are satisfied. We have solved the problem with  $N = 20$  and  $N = 40$  and summarise in Table 3.1 the convergence orders at the common nodes for  $p = 0, 1, 2$  according to equation (3.6). The orders agree remarkably with equation (3.6), the difference being attributed to numerical error. The global error is shown in Table 3.2 and illustrates the validity of equation (3.7).

$x_j$	$n^p(h)$			$x_j$	$n^p(h)$		
	$p = 0$	$p = 1$	$p = 2$		$p = 0$	$p = 1$	$p = 2$
0.05	6.0178	6.0180	6.0107	0.55	6.0102	6.0133	6.0231
0.10	6.0177	6.0151	6.0109	0.60	6.1360	6.0133	6.0130
0.15	6.0175	6.0146	6.0112	0.65	6.0155	6.0133	6.0116
0.20	6.0171	6.0144	6.0118	0.70	6.0166	6.0130	6.0113
0.25	6.0164	6.0143	6.0126	0.75	6.0172	6.0125	6.0114
0.30	6.0150	6.0142	6.0142	0.80	6.0175	6.0105	6.0117
0.35	6.0125	6.0142	6.0185	0.85	6.0177	6.0442	6.0123
0.40	6.0082	6.0142	6.0543	0.90	6.0177	6.0179	6.0134
0.45	6.0038	6.0146	6.9835	0.95	6.0177	6.0174	6.0163
0.50	6.0053	6.0119	6.9829				

Table 3.1: Nodal convergence rates.

$p$	$n^p(h)$
0	6.0214
1	5.0000
2	4.0125
3	2.9963

Table 3.2: Global convergence rates.

#### 4. APPLICATION TO PDES, BURGERS' AND KDV EQUATIONS

We consider the solution of PDEs, in space and time, by collocation. To simplify the explanation, we consider one spatial variable and apply collocation in this variable. It is possible to solve both linear and non-linear systems. Firstly, we illustrate examples for a linear system and

then, as a nonlinear application, we consider the Burgers' and KdV equations. We consider the following third order PDE:

$$(4.1) \quad u_t + \mu u_{xxx} + \nu u_{xx} + \varepsilon uu_x = f(x), \quad x \in (a, b), \quad t \geq 0,$$

$$(4.2) \quad u(a, t) = g_1(t), \quad u(b, t) = g_2(t), \quad u_x(a, t) = g_3(t),$$

where  $\mu$ ,  $\nu$  and  $\varepsilon$  are non-negative constants and the PDE is augmented with three boundary conditions at  $x = a$ ,  $x = b$  together with an initial condition at  $t = 0$ , which are well defined. Analogous to equation (3.3), the trial solution, in the  $i_{th}$  element, is written as

$$(4.3) \quad U^i(z, t) = \sum_{k=1}^6 a_{k+3(i-1)}(t) H_k(z).$$

Here the time dependence is reflected in the coefficients  $a$ . Substituting (4.3) into (4.1), we obtain

$$(4.4) \quad \sum_{k=1}^6 a'_{k+3(i-1)}(t) H_k(z) + \frac{\mu}{h^3} \sum_{k=1}^6 a_{k+3(i-1)}(t) H_k'''(z) + \frac{\nu}{h^2} \sum_{k=1}^6 a_{k+3(i-1)}(t) H_k''(z) + \frac{\varepsilon}{h} \sum_{k=1}^6 a_{k+3(i-1)}(t) H_k(z) H_k'(z) = f(z).$$

The boundary conditions (4.2) imply that  $a_1(t) = g_1(t)$ ,  $a_{3N+1}(t) = hg_2(t)$  and  $a_2(t) = g_3(t)$ . We then substitute three collocation points from each sub-interval into equation (4.4) to obtain  $3N$  conditions. Using these, along with the boundary conditions, we get a linear differential algebraic system of size  $3N + 3$ , which is solved with DASSL subroutine in Julia. We also note the method is computationally more efficient than other similar implementations in which Hermite polynomials [4, 5], is used which uses four collocation points in each subinterval as compared to three collocation points per subinterval required here.

We consider two linear third order PDEs with known exact solution.

**Example 4.1.** We take  $\nu = \varepsilon = 0$ ,  $\mu = -1$  and  $x \in [0, 1]$ . The exact solution and resulting source term is given by

$$u(x, t) = \cos(t) \sin(3\pi x), \quad f(x, t) = 27\pi^3 \cos(t) \cos(3\pi x) - \sin(t) \sin(3\pi x).$$

The graphs of both the solution and error are depicted in the top left and right panels in Figure 4, respectively. The numerical results indicate that the present method is successful in capturing the oscillatory nature of the solution in both space and time with a reasonable accuracy. The drop in accuracy as compared to the ode case can be attributed to the error in the time integration process.

**Example 4.2.** We take  $\nu = \varepsilon = 0$ ,  $\mu = -1$  and  $x \in [0, 1]$ . The exact solution and resulting source term is given by

$$u(x, t) = e^{-t} \sin(3\pi x), \quad f(x, t) = 27\pi^3 e^{-t} \cos(3\pi x) - e^{-t} \sin(3\pi x).$$

The solution and error graphs are shown in the bottom left and right panels in Figure 4, respectively. In this case, the solution decays exponentially. We consider the nonlinear Burgers' equation ( $\varepsilon = 1$ ,  $\nu = -1$ ,  $\mu = 0$ ). Since there are two boundary conditions we use one additional collocation point in the first subinterval.



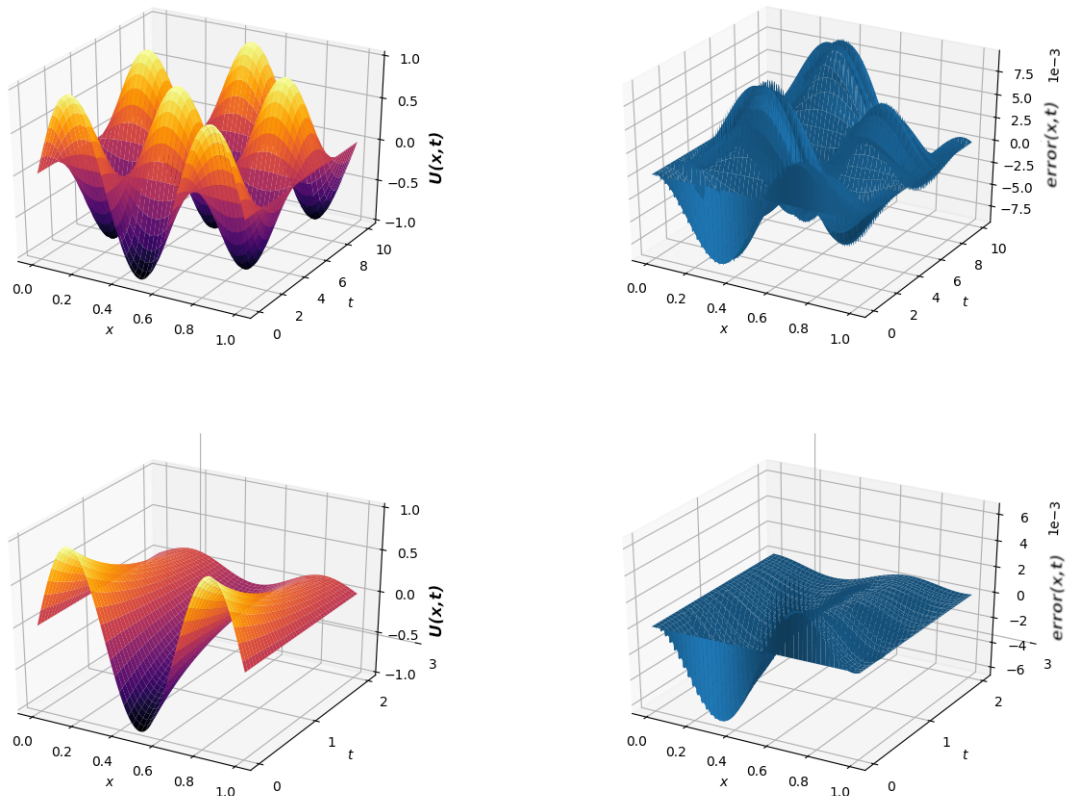


Figure 4: Left panel: Numerical solution. Right panel: Error

**Example 4.3.** We take  $x \in [0, 1]$ ,  $t \geq 1$  and the exact solution is given by, (see [1])

$$u(x, t) = \frac{\frac{x}{t}}{1 + \left(\frac{t}{t_0}\right)^{\frac{1}{2}} \exp\left(\frac{x^2}{4\nu t}\right)}, \quad t_0 = \frac{1}{8\nu}.$$

We substitute the  $3N + 1$  collocation points into (4.4) to obtain a  $(3N + 1) \times (3N + 1)$  matrix vector system whose solution yields the value of the coefficients at  $t = 1$ . In a similar manner, by setting  $u_t(z, 1) = U_t(z, 1)$  we obtain the derivatives of the coefficient initially. These values are required by the differential algebraic solver, DASSL, in order to solve for the time profile of the coefficients. Thereafter the PDE solution over the domain is obtained from equation (4.3). The solution and the error are shown in the left and right panels in Figure 5, respectively. This example describes a wave propagating to the right. The spikes in the error graph occur precisely where the peaks are located in the solution graph. The error, however, is acceptable as it is of the order  $10^{-4}$ .

**Example 4.4.** We consider  $x \in [-10, 10]$ ,  $t \geq 0$ . The exact solution is chosen to illustrate the travelling wave solution case

$$(4.5) \quad u(x, t) = \frac{1}{3 \left(1 + e^{\frac{6x-t}{36\nu}}\right)}.$$

The graphs of both the solution and the error are depicted in the left and right panels Figures 5, respectively. The solution and error behave in a similar manner to that of example 3, however the error is an order of magnitude better.

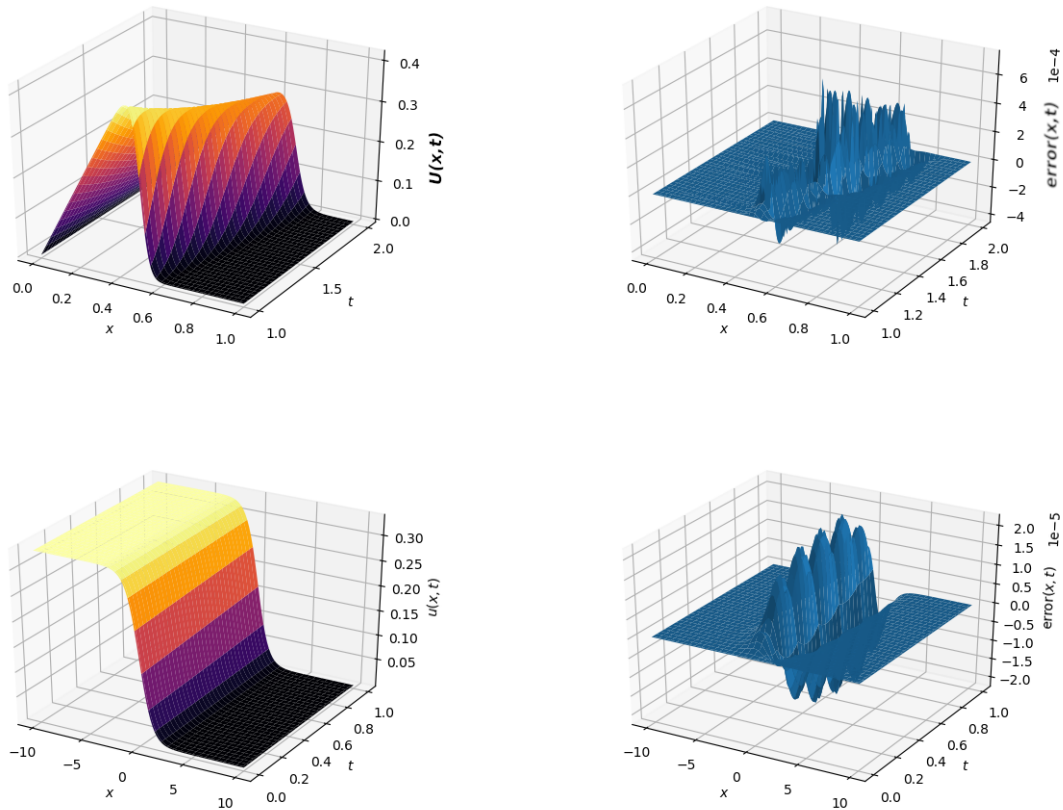


Figure 5: Left panel: Numerical solution. Right panel: Error

**Example 4.5.** As the final example we consider  $\nu = 0$ ,  $\varepsilon = 6$  and  $f(x, t) = 0$  in (4.1) which corresponds to the nonlinear KdV equation.

Here we consider an alternative strategy for performing the time integration, namely the quasilinearization method. Equation (4.1) is integrated on  $[t_j, t_{j+1}]$  using the trapezoidal rule and the non-linear term is linearized with respect to time, to yield

$$(4.6) \quad \left[ 1 + \frac{\varepsilon \Delta t}{2} u_x(x, t_j) \right] u(x, t_{j+1}) + \frac{\varepsilon \Delta t}{2} u(x, t_j) u_x(x, t_{j+1}) + \mu \frac{\Delta t}{2} u_{xxx}(x, t_{j+1}) = u(x, t_j) - \mu \frac{\Delta t}{2} u_{xxx}(x, t_j)$$

Transforming to  $z$  and substituting (3) into (5), we get

$$\sum_{k=1}^6 \left( \left[ 1 + \frac{\varepsilon \Delta t}{2h} \sum_{k=1}^6 a_{k+3(i-1)}(t_j) H'_k(z) \right] H_k(z) + \left[ \frac{\varepsilon \Delta t}{2h} \sum_{k=1}^6 a_{k+3(i-1)}(t_j) H_k(z) \right] H'_k(z) + \mu \frac{\Delta t}{2h^3} H'''_k(z) \right) a_{k+3(i-1)}(t_{j+1}) = \sum_{k=1}^6 \left[ H_k(z) - \mu \frac{\Delta t}{2h^3} H'''_k(z) \right] a_{k+3(i-1)}(t_j).$$

We choose three collocation points in the  $N$  intervals and substitute into equation (6). The points are chosen as the Gauss points shifted to the interval  $[0, 1]$ . Together with the three boundary conditions we obtain a  $(3N + 3) \times (3N + 3)$  linear system of the form

$$M \mathbf{a}^{j+1} = B \mathbf{a}^j$$

where  $\mathbf{a}^{j+1}$  is the vector of unknown coefficients at time  $t_{j+1}$ . We determine  $\mathbf{a}^0$  from the initial condition

$$(4.7) \quad \begin{aligned} u(z, t_0) &= U(z, t_0) \\ &= \sum_{k=1}^6 a_{k+3(i-1)}(t_0) H_k(z), \end{aligned}$$

by substituting the collocation points into equation (4.7) and solving the resulting linear system. The exact solution is taken as

$$(4.8) \quad u(x, t) = \frac{36 + 48 \cosh(2x - 8t) + 12 \cosh(4x - 64t)}{(3 \cosh(x - 28t) + \cosh(3x - 36t))^2}$$

which corresponds to the 2-soliton case [12]. The numerical solution and error are illustrated in Figure 6. It is seen that the OCFE algorithm is successful in capturing the solitary waves. The drop in the error can be attributed to the time integration process.

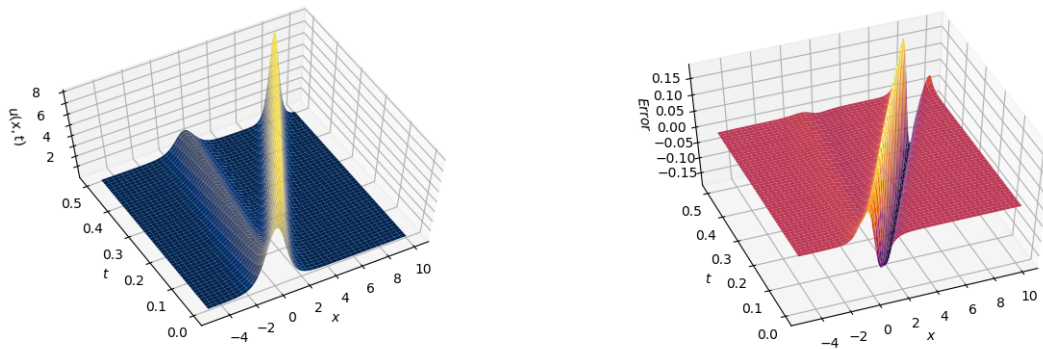


Figure 6: Left panel: Approximate solution Right panel: Error  $N = 100, \nu = 0.1$

### 5. CONCLUSION

In this paper we have systematically presented the OCFE method using quintic  $C^2$  Hermite splines. The method is suitable for solving third order BVPs and PDEs and seems to be the optimal method in the class of piecewise splines collocation methods. We have demonstrated the applicability and efficiency of the method on a wide class of problems including traveling wave and soliton solutions of the Burgers' and KdV equations. Further, the method should be suitable for solving problems in engineering applications involving steep solution profiles and moving fronts. The present implementation is based on quintic polynomials but can be readily extended to higher order polynomials. The use of Heptic (seventh order) splines is presently under investigation.

### REFERENCES

[1] A. H. A. ALI, G. A. GARDNER and L. R. T. GARDNER, A collocation solution for Burgers' equation using cubic B-spline finite elements, *Appl. Math. Comput.*, **100** (1992), pp. 325–337.  
 [2] S. ARORA, S. S. DHALIWAL and V. K. KUKREJA, Solution of two point boundary value problems using orthogonal collocation on finite elements, *Appl. Math. Comput.*, **171(1)** (2005), pp. 358–370.

- [3] S. ARORA , S. S. DHALIWAL and V. K. KUKREJA, Simulation of washing of packed bed of porous particles by orthogonal collocation on finite elements, *Comput. Chem. Eng.*, **30(6-7)** (2006), pp. 1054–1060.
- [4] S. ARORA and I. KAUR, An efficient scheme for numerical solution of Burgers' equation using quintic Hermite interpolating polynomials, *Arab. J. Math.*, **5** (2016), pp. 23–34.
- [5] S. ARORA, R. JAINA and V. K. KUKREJA, Solution of Benjamin-Bona-Mahony-Burgers' equation using collocation method with quintic Hermite splines, *Appl. Numer. Math.*, **154** (2020), pp. 1–16.
- [6] B. BIALECKI and G. FAIRWEATHER, Orthogonal spline collocation methods for partial differential equations, *J. Comput. Appl. Math.*, **128** (2001), pp. 55-82.
- [7] B. BIALECKI and N. FISHER, Maximum norm convergence analysis of extrapolated Crank-Nicolson orthogonal spline collocation for Burgers' equation in one space variable, *J. Differ. Equ. Appl.*, **24(10)** (2018), pp. 1621–1642.
- [8] C. J. BANSILAL, *Numerical Solution of Differential Equations Using Quintic Hermite Collocation*, University of KwaZulu-Natal, Durban, 2020.
- [9] C. DE BOOR and B. SWARTZ, Collocation at Gaussian points, *SIAM J. Numer. Anal.*, **10** (1973), pp. 582–606.
- [10] H. BRUNNER and H. ROTH, Collocation in space and time: experience with the Korteweg-de Vries equation, *Appl. Numer. Math.*, **25** (1997), pp. 369–390.
- [11] G. F. CAREY and B. A. FINLAYSON, Orthogonal collocation on finite elements, *Chem. Eng. Sci.*, **30** (1975), pp. 587–596.
- [12] J. M. CURRY, Soliton solutions of integrable systems and Hirota's method, *H. C. M. R.*, **2(1)** (2008), pp. 43–59.
- [13] J. DOUGLAS and T. DUPONT, A finite element collocation method for quasilinear parabolic equations, *Math. Comp.*, **27** (1973), pp. 17–28.
- [14] J. DOUGLAS and T. DUPONT, *Collocation Methods for Parabolic Equations in a Single Space Variable Based on  $C1$  Piecewise-polynomial Spaces*, Springer, Berlin, 1974.
- [15] B. A. FINLAYSON, Orthogonal collocation on finite elements- progress and potential, *Math. Comput. Simulat.*, **XXII** (1980), pp. 11–17.
- [16] I. A. GANAIE, B. GUPTA, N. PARUMASUR, P. SINGH and V. K. KUKREJA, Asymptotic convergence of cubic Hermite collocation method for parabolic partial differential equation, *Appl. Math. Comput.*, **220** (2013), pp. 560-567.
- [17] A. K. MITTAL, I. A. GANAIE, V. K. KUKREJA, N. PARUMASUR and P. SINGH, Solution of diffusion–dispersion models using a computationally efficient technique of orthogonal collocation on finite elements with cubic Hermite as basis, *Comput. Chem. Eng.*, **58** (2013), pp. 203-210.